Magnetocaloric and magnetic properties of La_2NiMnO_6 double perovskite

Masrour R† and Jabar A

Laboratory of Materials, Processes, Environment and Quality, Cady Ayyed University, National School of Applied Sciences, P. O. Box 63 46000, *Safi, Morocco*

(Received 6 February 2016; revised manuscript received 30 March 2016; published online 25 June 2016)

The magnetic effect and the magnetocaloric effect in La_2NiMnO_6(LNMO) double perovskite are studied using the Monte Carlo simulations. The magnetizations, specific heat values, and magnetic entropies are obtained for different exchange interactions and external magnetic fields. The adiabatic temperature is obtained. The transition temperature is deduced. The relative cooling power is established with a fixed value of exchange interaction. According to the master curve behaviors for the temperature dependence of $\Delta S_m^{\max}$ predicted for different maximum fields, in this work it is confirmed that the paramagnetic–ferromagnetic phase transition observed for our sample is of a second order. The near room-temperature interaction and the superexchange interaction between Ni and Mn are shown to be due to the ferromagnetism of LNMO.

Keywords: oxides magnetocaloric, Monte Carlo simulation specific heat, magnetic properties

PACS: 75.30.Sg, 05.10.Ln **DOI:** 10.1088/1674-1056/25/8/087502

1. Introduction

Double perovskite of the general formula $A'A''B'B''X_6$; where the $(A'A'')$-sites are occupied by rare or alkaline earth ions, $(B'B'')$-sites by transition metal ions and (X)-sites by oxygen or halide ions, have been known for several decades.[1,2] The structure, magnetic, and dielectric properties of the double perovskite oxides, R_2NiMnO_6 ($R =$ Pr, Nd, Sm, Gd, Tb, Dy, Ho, and Y) are investigated in Ref. [3]. La_2NiMnO_6, exhibiting a ferromagnetic Curie temperature T_C of 280 K, has received considerable attention recently,[4–7] not only because of the possibility of combining multiple electronic properties (ferromagnetism, magnetoresistance, magneto capacitance, and semiconductivity) in this material, but also because of the expectation that a fundamental understanding of the Ni^{2+}–O–Mn^{4+} electronic interaction would provide new guidelines for designing the multiple property materials. The structural, electronic, and magnetic properties of the double perovskite Pb_2FeReO_6 have been studied by using the first principles.[8] The magnetic ordering was explained as the superexchange interaction between Ni^{2+}(d^8, $S = 1$) and Mn^{4+} (d^3, $S = 3/2$) ions.[7,9] Compared with other ferromagnetic semiconductors and insulators which only exhibit magnetic ordering at very low temperatures, La_2NiMnO_6 demonstrates ferromagnetic ordering near room temperature, as high as 280 K.[4,10] The magnetic hysteresis displacement, thermal inversion of the magnetization, hysteresis loops jumps, and crossing branches of hysteresis loops at low magnetic fields are reviewed.[11] The electronic and magnetic structures for the ferromagnetic and antiferromagnetic states of La_2MnNiO_6 and the site-projected density of states and electronic dispersion curves are analyzed in Ref. [12]. La_2NiMnO_6 is a ferromagnetic insulator with a positive superexchange interaction between Ni and Mn cations.[5,6,13–15] The influences of bismuth on the magnetic and electrical properties of La_2MnNiO_6 are studied in Ref. [16]. The Monte Carlo data by finite-size scaling, and the location of a line of critical points of the Ising universality class are analyzed.[17] The magneto-caloric effect of a $Gd_{55}Co_{25}Al_{18}Sn_2$ bulk metallic glass is investigated.[18] The crystal field and external magnetic field-split ground state of Dy^{3+} in $Dy_3Al_5O_{12}$ are calculated based on the quantum theory.[19] In this paper, theoretical work on the dependence of the magnetization on temperature for La_2MnNiO_6 compound is simulated to predict magnetocaloric properties such as magnetic entropy change, relative cooling power, and heat capacity change. The thermal magnetization, $\mathrm{d}M/\mathrm{d}T$, specific heat, and magnetic entropy are given for a fixed magnetic parameter. The transition temperature T_C values of La_2NiMnO_6 double perovskite are deduced for different values of external magnetic field. The thermal total magnetization, specific heat, and magnetic entropy are established with the external magnetic field h. We also give the adiabatic temperatures with different values of external magnetic field. Finally, the field dependence of relative cooling power (RCP) is obtained.

2. Model and formulation

The Hamiltonian of an Ising model with the La_2NiMnO_6 double perovskite includes nearest neighbor interactions and external magnetic field and is given as

$$H = -\sum_{\langle i,j\rangle} J_{ij(\mathrm{Ni-Ni})}\sigma_i\sigma_j - \sum_{\langle i,j\rangle} J_{ij(\mathrm{Mn-Mn})}S_iS_j - \sum_{\langle i,j\rangle} J_{ij(\mathrm{Mn-Ni})}S_i\sigma_j - h\sum_i(\sigma_i + S_i), \quad (1)$$

†Corresponding author. E-mail: rachidmasrour@hotmail.com

© 2016 Chinese Physical Society and IOP Publishing Ltd

where $\langle i, j\rangle$ denote the first and second nearest neighbor sites i and j; h is the external magnetic field; $J_{ij\,(\mathrm{Ni-Ni})}$, $J_{ij\,(\mathrm{Mn-Mn})}$, $J_{ij\,(\mathrm{Mn-Ni})}$ are the first ($J_{1\,(\mathrm{Ni-Ni})}$, $J_{1\,(\mathrm{Mn-Mn})}$, $J_{1\,(\mathrm{Mn-Ni})}$) and second $J_{2\,(\mathrm{Ni-Ni})}$, $J_{2\,(\mathrm{Mn-Mn})}$, $J_{2\,(\mathrm{Mn-Ni})}$ nearest neighbor between the NiNi, MnMn, and MnNi respectively. The spin moments of Mn^{4+} and Ni^{2+} ions are $S = 3/2$ and $\sigma = 1$, respectively. We use the mean field theory to calculate the exchange interactions between Ni–Ni, Mn–Mn, and Mn–Ni. The obtained values are $J_{1\,(\mathrm{Ni-Ni})} = 22.0$ K, $J_{1\,(\mathrm{Mn-Mn})} = 24$ K, $J_{2\,(\mathrm{Ni-Ni})} = 19.0$ K, $J_{2(\mathrm{Mn-Mn})} = 23.0$ K, $J_{1\,(\mathrm{Mn-Ni})} = 15.0$ K, and $J_{2\,(\mathrm{Mn-Ni})} = 10.0$ K. The values of spin moment S and σ take $\pm 3/2$; $\pm 1/2$, and $\pm 1, 0$, respectively.

3. Monte Carlo simulations

The La_2NiMnO_6 double perovskite as given in Fig. 1 is assumed to reside in the unit cell and the system consists of the total number of spins $N = N_{\mathrm{Mn}} + N_{\mathrm{Ni}}$, with $N_{\mathrm{Mn}} = N_{\mathrm{Ni}} = 1024$.

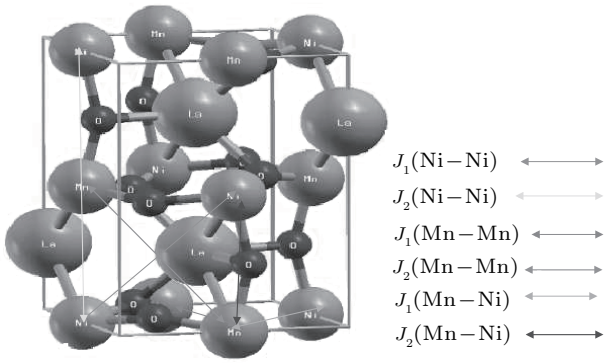


Fig. 1. Double perovskite La_2NiMnO_6 structure.

We use a standard sampling method to simulate the Hamiltonian given by Eq. (1). Cyclic boundary conditions on the lattice are imposed and the configurations are generated by sequentially traversing the lattice and making single-spin flip attempts. The flips are accepted or rejected according to a heat-bath algorithm under the Metropolis approximation. Our data are generated with 10^5 Monte Carlo steps per spin, discarding the first 10^4 Monte Carlo simulations. Starting from different initial conditions, we perform the average of each parameter and estimate the Monte Carlo simulations, averaging over many initial conditions. Our program calculates the following parameters:

(i) the magnetizations of Mn^{4+} and Ni^{2+} in La_2NiMnO_6 double perovskite

$$M_S = \left\langle \frac{1}{N_{\mathrm{Mn}}} \sum_i S_i \right\rangle, \tag{2}$$

$$M_\sigma = \left\langle \frac{1}{N_{\mathrm{Ni}}} \sum_i \sigma_i \right\rangle; \tag{3}$$

(ii) the total magnetization

$$M = \frac{M_S + M_\sigma}{2}, \tag{4}$$

where $N = N_{\mathrm{Mn}} + N_{\mathrm{Ni}}$;

(iii) the internal energy per site:

$$E = \frac{1}{N} \langle H \rangle; \tag{5}$$

(iv) the specific heat of La_2NiMnO_6:

$$C_m = \frac{\beta^2}{N} \left(\langle H^2 \rangle - \langle H \rangle^2 \right), \tag{6}$$

where $\beta = 1/k_{\mathrm{B}}T$ with T being the absolute temperature and k_{B} being the Boltzmann constant;

(v) the magnetic entropy:

$$S_m(T,h) = \int_0^T \frac{C_{p,h}}{T} \mathrm{d}T \tag{7}$$

with $C_{p,h}$ being the total specific heat as given by the Debye model and Debye + Einstein model:

$$C_{p,h} = 7.378T + 0.115T^3 + C_m \tag{8}$$

with the first two terms on the right-hand side being the usual electronic and lattice terms and the third term being the contribution from the magnetic structure;

(vi) the magnetic entropy change:

$$\Delta S_m(T,h) = \int_0^{h_{\max}} \left(\frac{\partial M}{\partial T} \right)_{h_i} \mathrm{d}h \tag{9}$$

with $h_{\max}$ being the maximum applied field, and $(\partial M/\partial T)_{h_i}$ being the thermal magnetization for a fixed magnetic field h_i;

(vii) the adiabatic temperature from Eq. (7):

$$\Delta T_{\mathrm{ad}} = -T \frac{\Delta S_m}{C_{p,h}}. \tag{10}$$

The defined parameter of RCP described as an area under the dependence of $\Delta S_m(T)$ on temperature, is a compromise between the magnitude of the magnetic entropy change and the width of the peak. The expression of relative cooling power RCP is

$$\mathrm{RCP} = \int_{T_1}^{T_2} \Delta S_m(T) \, \mathrm{d}T, \tag{11}$$

where T_1 and T_2 are the cold temperature and the hot temperature corresponding to both ends of the half-maximum value of $\Delta S_m^{\max}$, respectively.

4. Results and discussion

In a previous work, we have studied the magnetocaloric effect in $NdMnO_3$ perovskite by using the Monte Carlo simulations.[20] La_2NiMnO_6 is a double perovskite structure and is so named because the unit cell is twice that of perovskite. They do not have the same structures. In $NdMnO_3$, we consider the first nearest neighbor but in the La_2NiMnO_6 system we consider the first and the second exchange interactions for each atom.

Shown in Fig. 2(a) are the thermal total magnetizations of La_2NiMnO_6 and thermal magnetization of Ni and Mn. The dM/dT, specific heat, and magnetic entropy of La_2NiMnO_6 are given in Figs. 2(b)–2(d), respectively under $h = 0$. The ferromagnetic (FM) transition temperature is calculated from the minimum position of the (dM/dT) versus temperature curve. The observed ferromagnetism could be explained within the framework of FM interaction between the Mn and Ni ions.[6] The transition temperature obtained is $T_C = 275$ K. The transition from a paramagnetic (PM) state to an FM state around $T_C \approx 275$ K for the parent phase as reported in Refs. [6] and [16]. The near room temperature interaction and superexchange interaction between Ni^{+2} and Mn^{+4} are shown to be due to the ferromagnetism of LNMO. This behavior is observed in the previous work.[21] The double perovskite La_2NiMnO_6 is ferromagnetic at transition temperature $T_C = 280$ K, which has been predicted according to the Goodenough–Kanamori rules and confirmed by the experimental data.[15,22–24]

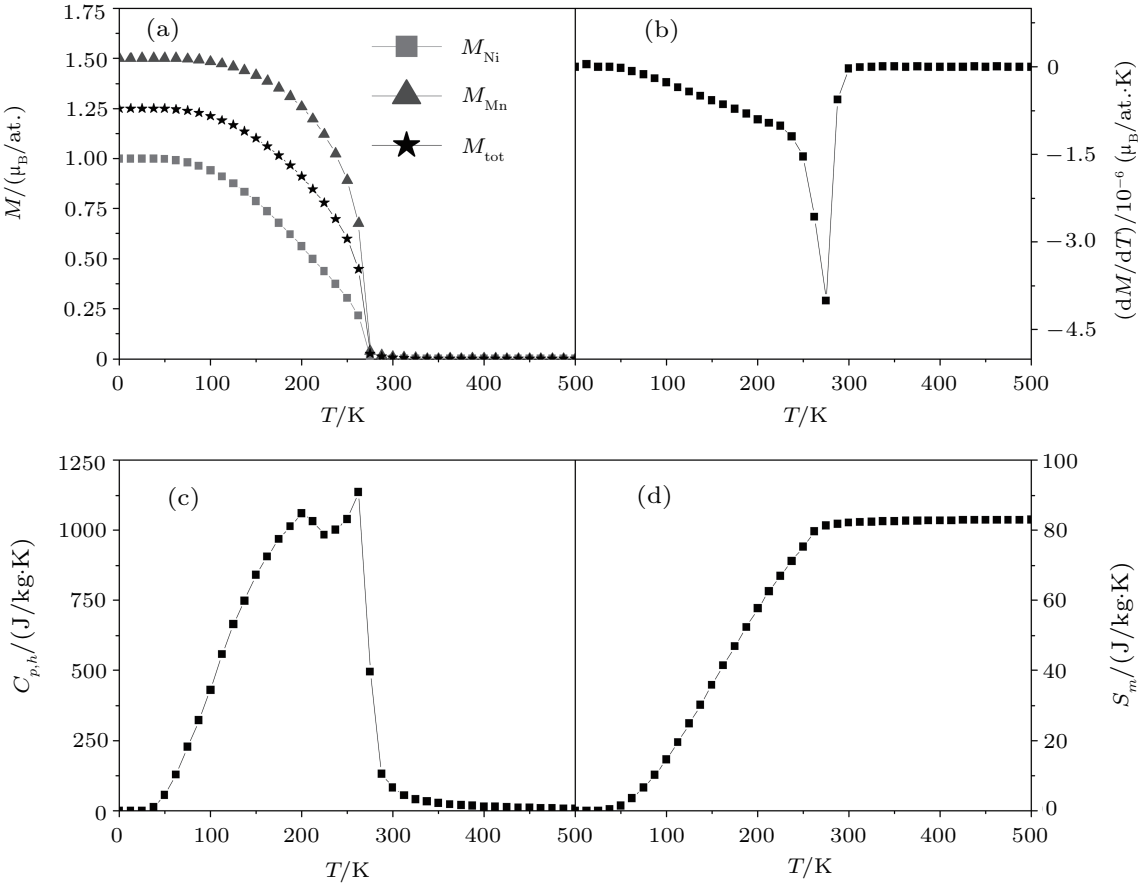


Fig. 2. Thermal magnetizations (a), dM/dT (b), the specific heat (c), and magnetic entropy (d) of La_2NiMnO_6 for $h = 0$.

The magnetic entropy increases with increasing temperature until the transition temperature T_C, which corresponds to the maximum value of the magnetic entropy. The thermal total magnetization and dM/dT of La_2NiMnO_6 are shown in Figs. 3(a) and 3(b), respectively for external magnetic field $h = 1, 4, 7$, and 10 T. The total magnetization increases with the external magnetic field increasing. On the other hand, Blasse argued that ferromagnetism in La_2NiMnO_6 is entirely due to Mn^{4+}–O–Ni^{2+} superexchange interactions,[16] which was later concluded[25] from the measurement of ^{55}Mn nuclear magnetic resonance line width. The curves of magnetic entropy versus the temperature of La_2NiMnO_6 are given in Fig. 4 for different values of external magnetic field $h = 1, 4, 7$, and 10 T. The magnetic entropy increases with increasing temperature until the transition temperature T_C and becomes constant for different values of external magnetic field.

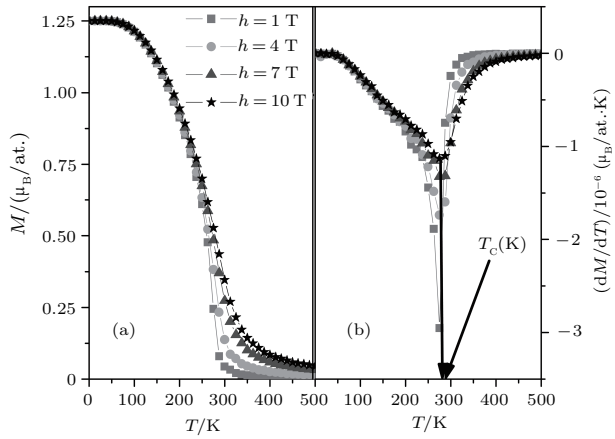


Fig. 3. Thermal total magnetizations (a) and dM/dT curves (b) of La_2NiMnO_6 for external magnetic field $h = 1$, 4, 7, and 10 T.

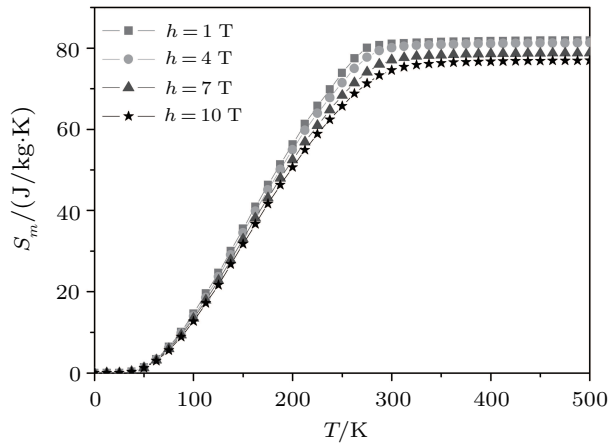


Fig. 4. Curves of magnetic entropy versus the temperature of La_2NiMnO_6 for different values of external magnetic field $h = 1$, 4, 7, and 10 T.

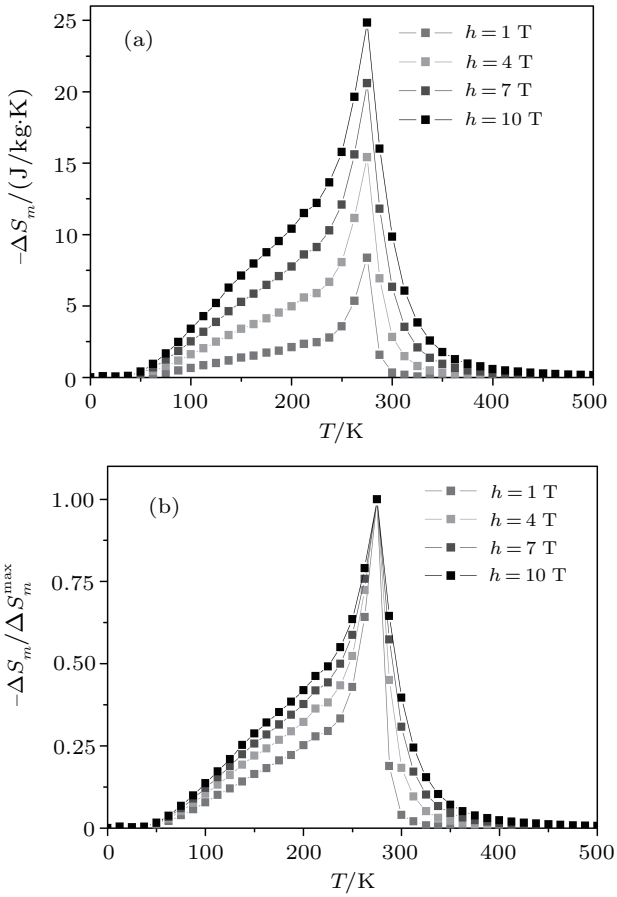


Fig. 5. Temperature dependences of the magnetic entropy change (a) and master curve behaviors of the curve each as a function of temperature (b) for $La_2NiMnO_6$for different values of external magnetic field $h = 1$, 4, 7, and 10 T.

We show in Fig. 5(a) the temperature dependences of the magnetic entropy for different values of external magnetic field $h = 1$, 4, 7, and 10 T. The value of ΔS_m is negative in the entire temperature range and is extended over a wide range of temperature around the Curie temperature, which is useful for above room temperature magnetic refrigeration. The values of $-\Delta S_m$ reach 8.44, 15.45, 20.65, and 25 J/(kg·K) at $T_C \approx 275$ K when the applied magnetic fields are 1, 4, 7, and 10 T, respectively. The paramagnetic–ferromagnetic transition is extremely sharp, indicating its second-order phase character as given in Fig. 5(b). One can see that all the $\Delta S_m(T,h)$ data points are collapsed into a universal curve in the whole temperature range as given in Ref. [26]. As is well known, the magnetic order is a second order phase transition in the La_2NiMnO_6. Therefore, the corresponding lattice and electronic entropy change will be much smaller. These also rule out the possibility that the magnetic entropy change is partially compensated for by the lattice and electronic contributions. This behavior is observed in previous work.[15]

A large change in magnetic entropy due to adiabatic magnetization is observed, which argues well for potential applications as magnetic refrigerant around liquid nitrogen temperature. Luo *et al*. suggested that the large magnetic entropy change in perovskite manganites could originate from the spin–lattice coupling in the magnetic ordering process.[27] We have also presented in Fig. 6, the temperature dependences of the adiabatic temperature in La_2NiMnO_6 for different values of external magnetic field $h = 1$, 4, 7, and 10 T. A large magnetic entropy change is observed and the changes of magnetic entropy and adiabatic temperature at moderate magnetic fields are quite significant. A maximum adiabatic temperature change about 275 K is obtained to be close to the transition temperature with applied field $h = 1$, 4, 7, and 10 T. These results indicate that our samples are very good substances for magnetic refrigeration applications. To explain a large magnetic entropy change in perovskite manganite, the Zener double exchange model has been strongly recommended.[28,29] A maximum entropy, $-\Delta S_M = 20.54\ \mathrm{J\cdot kg^{-1}\cdot K^{-1}}$ and adiabatic temperature change 4.84 K are comparable to these values: $35.5\ \mathrm{J\cdot kg^{-1}\cdot K^{-1}}$ ($\sim 24\ \mathrm{J\cdot kg^{-1}\cdot K^{-1}}$, and 10.5 K (6.5 K) is observed in Gd_2NiMnO_6 (Gd_2CoMnO_6) for a magnetic field change of 7 T at low temperatures.[30]

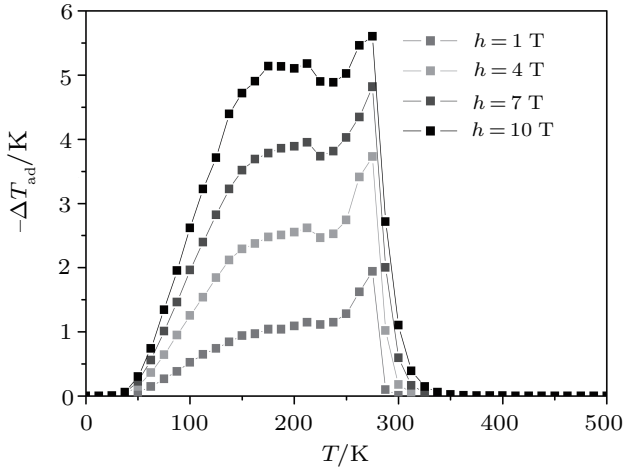


Fig. 6. Temperature dependences of the adiabatic temperature change for La_2NiMnO_6 for different values of external magnetic field $h = 1$, 4, 7, and 10 T.

Figure 7 shows the field dependence of relative cooling power (RCP) on external magnetic field for La_2NiMnO_6. It

can be seen from this figure that RCP increases monotonically as the field increases, and reaches the value of 905 J·kg for $h = 10$ T. The RCP is another important factor for assessing the usefulness of a magnetic refrigerant material.[31] The RCP depends not only on the magnitude of ΔS_m, but also on the temperature dependence of ΔS_m (e.g., the full width at half maximum of the $\Delta S_m^{\max}$).[32] The values obtained around $T_C = 275$ K increase with applied field increasing. All the parameters related to the magnetocaloric effect, such as the magnetic entropy change, relative cooling power, and refrigerant capacity depend strongly on the magnitude of the applied magnetic field h and exchange interaction between Mn and Ni ions.

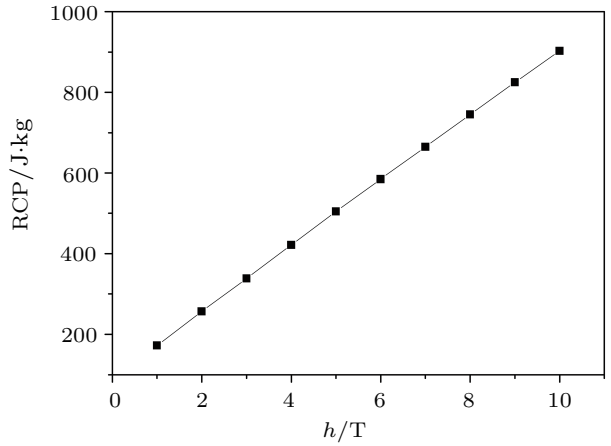


Fig. 7. Field dependence of relative cooling power (RCP) for La_2NiMnO_6.

Finally, we show in Fig. 8 the hysteresis loops of La_2NiMnO_6 for different temperatures $T = 260$, 275, and 285 K. The coercive field decreases with temperature increasing. The same behavior has been observed experimentally.[33] The system exhibits the superparamagnetic behavior for $T \geqslant T_C$. However, although the large abrupt change in magnetization causes correspondingly a giant magnetic entropy change, this appears at the expense of thermal and magnetic hysteresis, which should be avoided in order to be able to apply these materials in refrigerators appliances. The coercive field in this double perovskite is sample-dependent, which might indicate that the role of structural defects such as antiphase boundaries[34] acting as domain pinning centres can be very important in such highly anisotropic compounds. Antiphase boundaries in double perovskite can occur when there appears a lattice shift equal to half a lattice parameter along a crystallite plane. This gives rise to a plane formed by antiferromagnetic Ni–O–Ni bonds or Mn–O–Mn bonds. The extremely large magnetic entropy change may be attributed to a large number of weakly interacting spins. These indicate that the material is a promising magnetocaloric effect (MCE) candidate for low temperature application, and possibly could make ultra-low temperatures easily achievable for most laboratories and for space application as well.

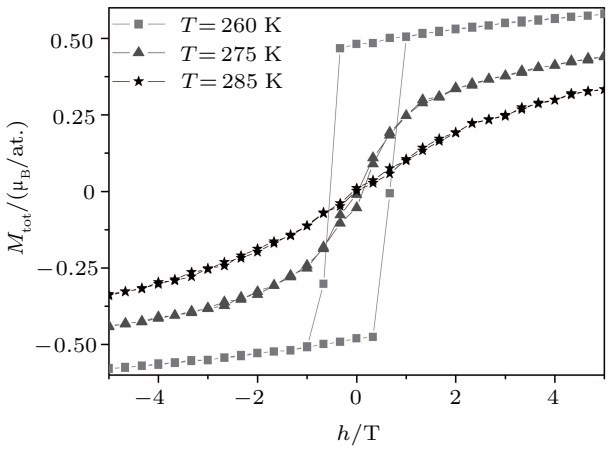


Fig. 8. Hysteresis loops of La_2NiMnO_6 for different temperatures $T = 260$, 275, and 285 K.

5. Conclusions

The magnetocaloric effect and the critical behavior of the double perovskitesLa_2NiMnO_6 are investigated by Monte Carlo simulations. The maximum of the magnetocaloric effect corresponds to transition temperature T_C. The La_2NiMnO_6 shows the second order PM–FM phase transition around 12 with a large magnetic entropy change over a wide range of temperature, which is comparable to the magnetic entropy changes of other manganites. The changes in magnetic entropy and the adiabatic temperature are also significant at moderate magnetic fields. Therefore, a great deal of attention has been focused on finding new materials with a large MCE and small magnetic hysteresis.[35,36] These results are shown in our material. The exchange interaction between Mn–Ni atoms is the main mechanism that controls the magnetic and transport properties of manganite and are chosen the positive values as given in Refs. [5], [6], [13], and [15]. Finally, in order to study the nature of the paramagnetic–ferromagnetic phase transition, a master curve behavior for the temperature dependence of $\Delta S_m^{\max}$ predicted for different maximum fields is proposed and the hysteresis loop is obtained for the temperatures superior and inferior to those of the transition temperature.

References

[1] Flerov I N, Gorev M V, Aleksandrov K S, Tressaud A, Grannec J and Couzi M 1998 *Mater. Sci. Eng.* **24** 81
[2] Anderson M T, Greenwood K B, Taylor G A and Poeppelmeier K R 1993 *Prog. Solid State Chem.* **22** 197
[3] Booth R J, Fillman R, Whitaker H, Nag A, Tiwari R M, Ramanujachary K V, Gopalakrishnan J and Lofland S E 2009 *Mater. Res. Bull.* **44** 1559
[4] Rogado N S, Li J, Sleight A W and Subramanian M A 2005 *Adv. Mater.* **17** 2225
[5] Dass R I, Yan J Q and Goodenough J B 2003 *Phys. Rev. B* **68** 064415
[6] Joseph V L, Joy P A, Date S K and Gopinath C S 2002 *Phys. Rev. B* **65** 184416
[7] Sanchez M C, Garcia J, Blasco J, Subias G and Perez-Cacho J 2002 *Phys. Rev. B* **65** 144409
[8] Zhang Y, Ji V and Xu K W 2012 *Physica B* **407** 2617
[9] Wang T, Shi W Z, Fang X D, Dong W W and Tao R H 2010 *J. Sol–Gel Sci. Technol.* **53** 655

[10] Hashisaka M, Kan B, Masuno A, Takano M and Shimakawa Y 2006 *Appl. Phys. Lett.* **89** 032504
[11] Moure C and Pena O 2013 *J. Magn. Magn. Mater.* **337–338** 1
[12] Matar S F, Subramanian M A, Villesuzanne A, Eyert V and Whangbo M H 2007 *J. Magn. Magn. Mater.* **308** 116
[13] Goodenough J B, Wold A, Arnott R J and Menyuk N 1961 *Phys. Rev.* **124** 373
[14] Blasse G 1965 *J. Phys. Chem. Solids* **26** 1969
[15] Choudhury D, Mandal P, Mathieu R, Hazarika A, Rajan S, Sundaresan A, Waghmare U V, Knut R, Karis O, Nordblad P and Sarma D D 2012 *Phys. Rev. Lett.* **108** 127201
[16] Nautiyal P, Motin Seikh M, Pralong V and Kundu A K 2013 *J. Magn. Magn. Mater.* **347** 111
[17] Lv J P, Deng Y J and Chen Q H 2011 *Phys. Rev. E* **84** 021125
[18] Ding D, Zhang Y Q and Xia L 2015 *Chin. Phys. Lett.* **32** 106101
[19] Xue D, Ying Z G, Suo X W, Jia H Y and Feng H 2015 *Acta Phys. Sin.* **64** 177502 (in Chinese)
[20] Masrour R, Jabar A, Benyoussef A, Hamedoun M and Hlil E K 2016 *J. Magn. Magn. Mater.* **401** 91
[21] Zhou S, Shi L, Yang H and Zhao J 2007 *Appl. Phys. Lett.* **91** 172505
[22] Wang X, Sui Y, Li Y, Li X L, Wang Z Y, Liu Z, Su W and Tang J 2009 *Appl. Phys. Lett.* **95** 252502
[23] Wold A, Arnott R J and Goodenough J 1958 *Appl. Phys. Berl.* **29** 387
[24] Goodenough J B 1955 *Phys. Rev.* **100** 564
[25] Sonobe M and Asai K 1992 *J. Phys. Soc. Jpn.* **61** 4193
[26] Manh T V, Ho T A, Thanh T D, Phan T L, Phan M H and Yu S C 2015 *IEEE Trans. Magnetic.* **51** 2400304
[27] Luo X, Sun Y P, Wang B, Zhu X B, Song W H, Yang Z R and Dai J M 2009 *Solid State Commun.* **149** 810
[28] Guo Z B, Du Y W, Zhu J S, Huang H, Ding W P and Feng D 1997 *Phys. Rev. Lett.* **78** 1142
[29] Wang Z M, Ni G, Xu Q Y, Sang H and Du Y W 2001 *J. Appl. Phys.* **90** 5689
[30] Murthy K J, Chandrasekhar K D, Mahana S, Topwal D and Venimadhav A 2015 *J. Phys. D: Appl. Phys.* **48** 355001
[31] Tang T, Gu K M, Cao Q Q, Wang D H, Zang S Y and Du Y W 2000 *J. Magn. Magn. Mater.* **222** 110
[32] Kitanovski A and Egolf P W 2006 *Int. J. Refrig.* **29** 3
[33] Guo H Z, Burgess J, Ada E, Street S, Gupta A, Iliev M N, Kellock A J, Magen C, Varela M and Pennycook S J 2008 *Phys. Rev. B* **77** 174423
[34] Yu X, Asaka T, Tomioka Y, Tsuruta C, Naai T, Kimoto K, Kaneko Y, Tokura Y and Matsui Y 2005 *J. Electron Microsc.* **54** 61
[35] Cubrovic M, Zaanen J and Schalm K 2009 *Science* **325** 439
[36] Pfleiderer C, McMullan G J, Julian S R and Lonzarich G G 1997 *Phys. Rev. B* **55** 8330